Three-dimensional ordered macroporous Mn-Ce composite oxide catalysts with excellent low-temperature toluene oxidation performance: Synergistic effect and reaction mechanism

Siyuan Cheng[a,b], Ye Jiang[a,b,*], Guomeng Zhang[a,b], Yanan Liu[a,b], Xiao Dou[a,b], Xin Sun[a,b]

[a] *Shandong Key Laboratory of Hydrogen Energy Equipment and Safety, College of New Energy, China University of Petroleum (East China), 66 West Changjiang Road, Qingdao 266580, China.*

[b] *Qingdao Engineering Research Center of Efficient and Clean Utilization of Fossil Energy, Qingdao 266580, China*

[*] *Corresponding author*

Corresponding Author

Ye Jiang: jiangye@upc.edu.cn

Tel: 86-532-86981767

Fax: 86-532-86983683

Address: College of New Energy, China University of Petroleum (East China), 66 West Changjiang Road, Qingdao, P.R. China.

Experimental section

Preparation of PMMA template

Polymethyl methacrylate (PMMA) microspheres were prepared via soap-free emulsion polymerization. To begin the process, 650 mL of deionized water was placed in a 1000 mL three-neck flask, which was then positioned in a water bath. The entire reaction mixture was subsequently heated to 70°C. After the temperature stabilized, nitrogen was bubbled into the flask for 30 minutes to expel air. The electric stirrer was then turned on, and the stirring speed was maintained at 350 rpm. The reaction was maintained in a nitrogen atmosphere, and 55 mL of methyl methacrylate (MMA) was quickly poured into the flask and kept at 70°C for 15 minutes. The potassium persulfate initiator solution (0.2 g dissolved in 20 ml deionized water) preheated to 70°C was added. The solution appeared light blue and slowly turned milky white. After 40 minutes of constant temperature polymerization, a PMMA microsphere emulsion was obtained. Deionized water was used to dilute the PMMA microsphere emulsion to 2000 mL, resulting in a monodisperse PMMA microsphere emulsion. The PMMA template was obtained by centrifuging the monodisperse PMMA microsphere emulsion at 4000 r/min for 4 h, removing the supernatant, and drying at 80°C for 12 h.

Preparation of 3DOM Mn-Ce composite oxide catalysts

Specifically, an appropriate amount of $Ce(NO_3)_3$ $6H_2O$, 50 wt% $Mn(NO_3)_2$ aqueous solution·and citric acid were dissolved in a solvent mixture consisting of methanol and ethylene glycol. Stirring the mixture magnetically until full dissolution of all chemicals yielded a precursor solution with an overall metal concentration of 2 mol/L. The ratios of cerium to manganese in each solution were 1:1, 2:1, 3:1, 1:2, and 1:3, respectively. Two grams of the PMMA template were

introduced into the aforementioned solution and immersed under vacuum for 6 h. Vacuum filtration was used for solid-liquid separation, with the collected solids then dried at 60°C overnight. Lastly, the sample was heated in a tube furnace using a two-stage program with a heating rate of 1°C/min. The samples were first heated to 300°C under N_2 flow and held for 2 h, then cooled to ambient temperature. Subsequent calcination at 450°C for 5 h in air yielded the 3DOM Mn-Ce composite oxide catalysts, which were denoted as 3DOM-Mn1Ce1、3DOM-Mn1Ce2、3DOM-Mn1Ce3、3DOM-Mn2Ce1、3DOM-Mn3Ce1. In addition, 3DOM-MnO_x and 3DOM-CeO_2 samples were also prepared, and the specific steps are consistent with the above. The difference was that only 50 wt% $Mn(NO_3)_2$ aqueous solution and $Ce(NO_3)_3$ $6H_2O$ were added, respectively.

Preparation of bulk Mn1Ce2 catalyst

For comparison, the Mn1Ce2 composite oxide catalyst without a 3DOM structure was also synthesized via the citric acid sol–gel method. Specifically, 0.01 mol 50 wt% $Mn(NO_3)_2$ aqueous solution and 0.02 mol $Ce(NO_3)_3$ $6H_2O$ were dissolved in 10 ml deionized water. Under stirring conditions, 3.842 g citric acid was added to the above metal salt solution, and the mixture was evaporated in an 80°C water bath to remove excess water until a gel was formed. Then, it was dried at 60°C for 12 h to obtain a solid. The solid was then heated from room temperature to 450°C at a heating rate of 5°C/min in an air atmosphere, and calcined for 5 h to finally obtain the bulk Mn1Ce2 composite oxide catalyst (denoted as Mn1Ce2).

Characterizations

X-ray diffraction (XRD) patterns. The crystal structure was determined by X-ray diffraction (XRD) measurements (Rigaku, D/max-2500PC) with Cu Kα radiation (λ = 0.15406 nm). The XRD data were scanned in the 2θ range 10–90° with a rate of 5°/min.

Brunauer-Emmett-Teller (BET). The physical structure characteristics of different catalyst samples were analyzed and determined by the physical adsorption apparatus (Micromeritics ASAP 2460, USA). The catalyst was desorbed at 200°C for 4 h in a vacuum environment, followed by N_2 adsorption-desorption at liquid nitrogen temperature (-196°C) to collect its isothermal curves. The BET (Brunner-Emmet-Teller) method was used to get the difference. The BJH (Barret-Joyner-Halenda) model was used to calculate the pore size and volume of the catalyst.

Scanning electron microscopy (SEM). The morphology of the catalysts was captured using a field emission scanning electron microscope (FESEM) equipped with an Xplore energy-dispersive X-ray spectroscopy (EDS) system (TESCAN, MIRA LMS, Czech Republic).

X-ray photoelectron spectroscopy (XPS). The atomic concentration and chemical valence of the sample surface elements were measured by X-ray photoelectron spectroscopy (Escalab 250Xi X, Thermo Fisher Scientific, USA), with the excitation source of Al Kα radiation. A small amount of powder sample was first weighed, pressed, and glued on top of the double-sided tape, followed by vacuum extraction to keep the pressure below 7 Pa. The area where the sample was concentrated was selected for testing. The binding energy of the full spectrum of the catalyst surface and the elements (Mn 2p, Ce 3d, O 1 s) were calibrated with C1 s during the data analysis.

Temperature-programmed reduction of hydrogen (H_2-TPR). The H_2 temperature programmed reduction (Finesorb-3010 Chemisorption Analyzer) was carried out to analyze the reducibility of the samples with a thermal conductivity detector (TCD) to record the signal. The 50 mg sample was pretreated with He for 1 hour, then cooled to room temperature and subjected to a 5% H_2/He programmed warming reduction experiment. The flow rate was 30 mL·min^{-1}, the ramp rate was 10°C·min^{-1}, and the reduction temperature range was 100-900°C with the TCD detector.

Temperature-programmed desorption of oxygen (O_2-TPD). The O_2 temperature-programmed desorption (O_2–TPD) measurements were carried out on the apparatus same as that used in the H_2–TPR experiments. The samples were pretreated under He atmosphere at 300°C for 1h and then cooled to room temperature. 5% O_2/He was added for 1 hour. Before the sample was heated, a helium flow (30 mL·min^{-1}) was employed to remove the O_2 for 30 min. The test was carried out in a flow of 5% O_2/He (30mL·min^{-1}) from room temperature to 800°C at a heating rate of 10°C·min^{-1}.

Temperature-programmed desorption of toluene (Toluene-TPD). The Toluene temperature-programmed desorption (Toluene–TPD) measurements were performed on a Programmed heating device. The sample of 100 mg was pretreated under an N_2 atmosphere at 150°C for 1h and then cooled to room temperature. Toluene was added for 1 hour. Before the sample was heated, an N_2 flow (30 mL·min^{-1}) was employed to remove the toluene until the baseline was stable. Then it heated up to 500°C at a heating rate of 4°C·min^{-1}.

Temperature-programmed surface reaction of toluene (Toluene-TPSR). The Toluene temperature-programmed desorption (Toluene–TPD) measurements were performed on a Programmed heating device. The sample of 100 mg was pretreated under an N_2 atmosphere at 150°C for 1h and then cooled to room temperature. Toluene was added for 1 hour. Before the sample was heated, an N_2 flow (30 mL·min^{-1}) was employed to remove the toluene until the baseline was stable. Then oxygen was introduced and the temperature was increased to 500°C at a heating rate of 4°C·min^{-1}.

In-situ diffuse reflectance infrared Fourier transform spectroscopy (*In situ* DRIFTS). The in situ diffuse reflectance infrared Fourier transform spectroscopy (*in situ* DRIFTS) was collected on

an FTIR spectrometer Bruker VERTEX70 equipped with a Harrick DRIFT cell and an MCT detector in the range of 1000-4000 cm^{-1} with 128 scans at a resolution of 4 cm^{-1} using a CaF_2 window. The catalysts were pretreated using nitrogen (40 ml min^{-1}) at 300°C for 30 minutes to remove the adsorbed gas. After cooling down to 50°C, a background spectrum was collected in the N_2 atmosphere. Then, the reaction gas flow (800ppm toluene+N_2 balanced or 800ppm toluene+21% O_2+N_2 balanced) at a flow rate of 40 mL/min was injected for toluene adsorption experiments. The temperature was raised to 160°C and stabilized for 30 minutes following the adsorption experiment. It then heated up and recorded the spectra at each temperature point. The high-temperature reaction measurement followed a similar procedure to the adsorption experiment except that after pretreatment, the temperature was raised to 240°C.

Catalytic evaluation

The catalytic performance was assessed using a fixed-bed reactor. A mixture of 100 mg catalyst and 200 mg quartz sand was loaded into a quartz tube with a diameter (Φ) of 8 mm. To simulate the real conditions, the liquid-phase blowing method was used to bring out the toluene vapor from the reagent bottle containing toluene. The gas mixture was 1000 ppm toluene, 21 vol.% O_2, and balanced N_2. The total flow rate was 100 mL·min^{-1}, which corresponds to a WHSV of 60000 mL·g^{-1}·h^{-1}. In addition, the total flow rates were adjusted to 150 mL/min and 200 mL/min, respectively, and the corresponding weight hourly space velocity (WHSV) were 90000 mL·g^{-1}·h^{-1} and 120000 mL·g^{-1}·h^{-1}, respectively, to study the effect of WHSV on the catalytic performance. The concentrations of reactant and product of toluene catalytic combustion were detected online by a gas chromatograph (GC9790 Plus), which was coupled with FID (to measure the concentration of toluene) and TCD (to detect the concentration of CO_2).

The toluene conversion was calculated as follows:

$$C_{\text{toluene}} = \frac{[C_7H_8]_{in} - [C_7H_8]_{out}}{[C_7H_8]_{in}} \times 100\%$$

where $[C_7H_8]_{in}$ and $[C_7H_8]_{out}$ denote the toluene concentrations of inlet and outlet, respectively. And the yield of CO_2 was calculated using the following equations:

$$S_{CO_2} = \frac{[CO_2]_{out}}{7\left([C_7H_8]_{in} - [C_7H_8]_{out}\right)} \times 100\%$$

where $[CO_2]_{out}$ is the outlet CO_2 concentration, and This equation is based on the molar ratio of toluene (C_7H_8) to CO_2 is 1:7

Kinetic Measurement

The reaction rate (K, mol·g^{-1}·s^{-1}) of toluene oxidation was calculated according to the following equations:

$$K = \frac{\eta \cdot F}{\mathrm{m}}$$

where η is the toluene conversion, F denotes the flow of gaseous toluene molecules (mol·s^{-1}), and m is the weight of the catalyst (g).

The apparent activation energy (E_a) was measured with toluene conversion (less than 20%) using the Arrhenius equation：

$$\ln r = -\frac{E_a}{\mathrm{R}T} + \ln \mathrm{A}$$

where r is the rate system constant of the reaction, R is the ideal gas constant (8.314 J·mol^{-1}·K^{-1}), T is the reaction temperature (K), and A is the pre-exponential factor. Finally, the activation energy of the catalytic combustion of toluene with different catalysts can be found by plotting ln$r$~1000/T.

Figures and Tables

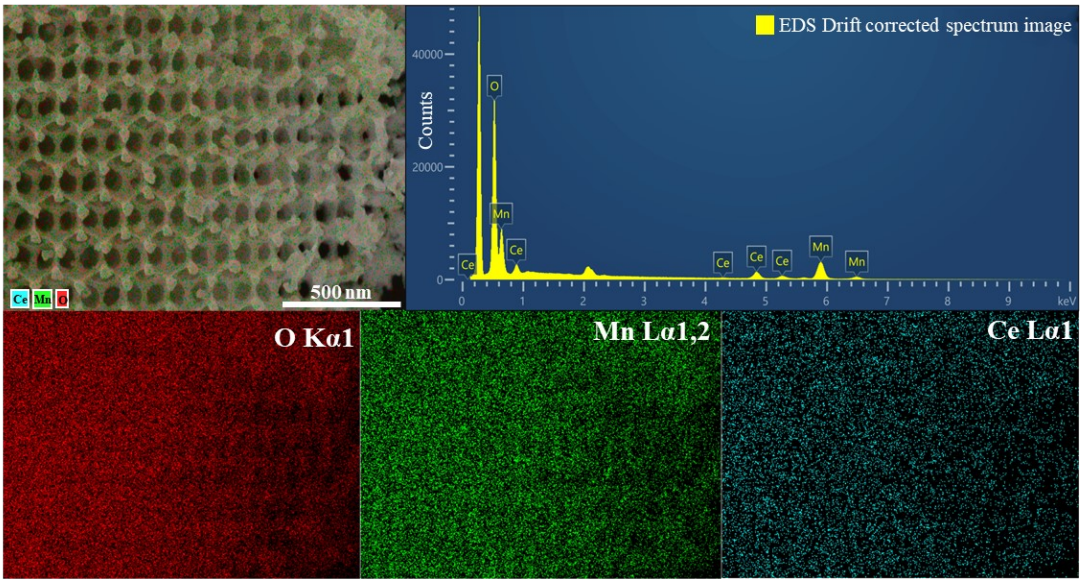

Fig. S1. EDS mapping images of 3DOM-Mn1Ce2 catalyst.

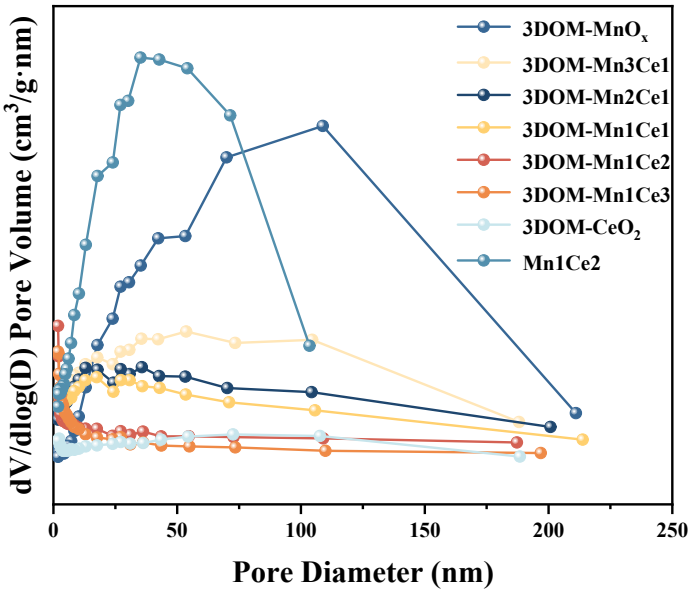

157

158 **Fig. S2.** Pore distributions of 3DOM-MnO_x, 3DOM-CeO_2, 3DOM Mn-Ce composite oxides, and
159 Mn1Ce2.

160

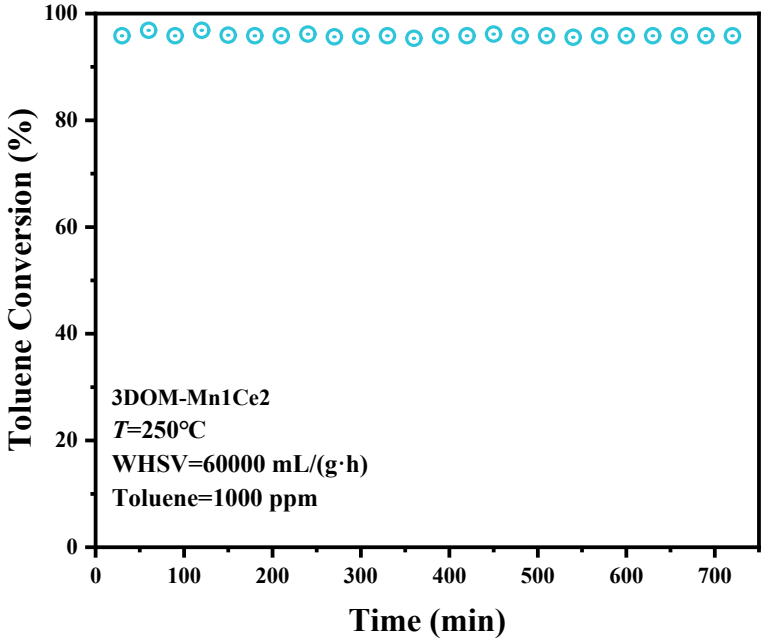

Fig. S3. long-term stability test of 3DOM-Mn1Ce2 catalyst for toluene oxidation.

Table S1 Textural Properties, XPS, Toluene-TPD results of the prepared catalysts

Catalyst	Pore volume (cm^3/g)[a]	Average pore size (nm)[a]	Ce^{3+}/Ce[b]	Mn^{4+}/Mn[b]	O_{ads}/O[b]	CO_2/toluene[c]
3DOM-MnO_x	0.135	25.91	——	0.18	0.48	8.07
3DOM-Mn3Ce1	0.099	11.49	0.17	0.24	0.49	9.88
3DOM-Mn2Ce1	0.083	10.45	0.15	0.22	0.48	9.13
3DOM-Mn1Ce1	0.076	8.86	0.17	0.26	0.49	10.17
3DOM-Mn1Ce2	0.061	6.26	0.19	0.32	0.54	14.27
3DOM-Mn1Ce3	0.052	5.52	0.18	0.28	0.51	10.29
3DOM-CeO_2	0.035	9.52	0.13	——	0.43	7.07
Mn1Ce2	0.198	15.09	0.14	0.19	0.46	7.86

a Pore volume and average pore size measured using the BJH method.

b The ratios of surface elements were obtained through XPS fitting analysis.

c The ratios of CO_2/toluene were determined according to the peak area ratio.

Table S2 Catalytic testing conditions (catalysts, space velocity, pollutant type and concentration) and catalytic activities (T_{90}) of as-prepared 3DOM-Mn1Ce2 catalyst and previously reported catalysts.

Catalysts	Space velocity mL/(g·h)	Pollutant	Concentration	T_{90} (°C)	Ref.
3DOM-LMO	120000	Toluene	2000 ppm	357	[1]
0.93Au/11.2MnO_x/3DOM SiO_2	20000	Toluene	1000 ppm	255	[2]
ESFO-3DOM	20000	Toluene	1000 ppm	305	[3]
$La_{0.9}Sr_{0.1}Co_{0.9}Mn_{0.1}O_3$	30000	Toluene	2000 ppm	328	[4]
3DOM Co_3O_4	40000	Toluene	1000 ppm	294	[5]
1.9Au/3DOM Mn_2O_3	40000	Toluene	1000 ppm	258	[6]
3DOM Mn_2O_3	40000	Toluene	1000 ppm	297	[6]
$LaMnO_3$-PL-2	20000	Toluene	1000 ppm	249	[7]
3DOM Mn_2O_3	40000	Toluene	1000 ppm	280	[8]
5.8Au/3DOM Mn_2O_3	40000	Toluene	1000 ppm	244	[9]
3Mn1Ce	60000	Toluene	1000 ppm	239	[10]
0.5Mn-0.5Ce	60000	Toluene	1000 ppm	250	[11]
MnCe	30000	Toluene	1000 ppm	254	[12]
3DOM Mn1Ce2	60000	Toluene	1000 ppm	244	This work

[1] W. Z. Si, Y. Wang, S. Zhao, F. Y. Hu and J. H. Li, *Environ. Sci. Technol.*, 2016, **50**, 4572-4578.

[2] H. G. Yang, J. G. Deng, S. H. Xie, Y. Jiang, H. X. Dai and C. T. Au, *Appl. Catal. A Gen.*, 2015, **507**, 139-148.

[3] K. M. Ji, H. X. Dai, J. G. Deng, H. Y. Jiang, L. Zhang, H. Zhang and Y. J. Cao, *Chem. Eng. J.*, 2013, **214**, 262-271.

[4] Z. Shi, F. Dong, Z. C. Tang and X. Y. Dong, *Chem. Eng. J.*, 2023, **473**, 145476.

[5] S. H. Xie, J. G. Deng, S. M. Zang, H. G. Yang, G. S. Guo, H. Arandiyan and H. X. Dai, *J. Catal.*, 2015, **322**, 38-48.

[6] S. H. Xie, J. G. Deng, Y. X. Liu, Z. H. Zhang, H. G. Yang, Y. Jiang, H. Arandiyan, H. X. Dai and C. T. Au, *Appl. Catal. A Gen.*, 2015, **507**, 82-90.

[7] Y. X. Liu, H. X. Dai, Y. C. Du, J. G. Deng, L. Zhang and Z. X. Zhao, *Appl. Catal. B Environ.*, 2012, **119**, 20-31.

[8] W. B. Pei, Y. X. Liu, J. G. Deng, K. F. Zhang, Z. Q. Hou, X. T. Zhao and H. X. Dai, *Appl. Catal. B Environ.*, 2019, **256**, 117814.

[9] S. H. Xie, H. X. Dai, J. G. Deng, H. G. Yang, W. Han, H. Arandiyan and G. S. Guo, *J. Hazard. Mater.*, 2014, **279**, 392-401.

[10] J. Chen, X. Chen, X. Chen, W. Xu, Z. Xu, H. Jia and J. Chen, *Appl. Catal. B Environ.*, 2018, **224**, 825-835.

[11] B. Yang, Y. Q. Zeng, M. J. Zhang, F. Y. Meng, Q. Zhong and S. L. Zhang, *J. Rare Earths*, 2023, **41**, 374-380.

[12] Y. Jiang, Y. Jiang, C. Su, X. Sun, Y. Xu, S. Cheng, Y. Liu, X. Dou and Z. Yang, *Fuel*, 2024, **355**, 129402.

Table S3 Multiple linear regression (MLR) analysis results for Ce^{3+}/Ce, Mn^{4+}/Mn, O_{ads}/O, BET surface area, and average crystallite size.

Physicochemical Parameters	Absolute value of β	p-value
BET surface area	0.827	0.022
Average crystallite size	0.308	0.502
Ce^{3+}/Ce	0.399	0.376
Mn^{4+}/Mn	0.999	0
O_{ads}/O	0.940	0.002

Table S4 Toluene-TPD peak area data

Catalysts	Toluene desorption peak area	CO_2 generation peak area	CO_2/toluene
3DOM-MnO_x	8189.66	26915.13	3.28
3DOM-Mn3Ce1	11801.65	41540.57	3.51
3DOM-Mn2Ce1	11198.13	38666.15	3.45
3DOM-Mn1Ce1	16018.49	58179.91	3.63
3DOM-Mn1Ce2	26049.34	101803.27	3.91
3DOM-Mn1Ce3	22347.18	82023.06	3.67
3DOM-CeO_2	8027.02	8206.26	1.02
Mn1Ce2	4663.88	14568.99	3.12

Table S5 Assignment of IR bands appearing after the adsorption-oxidation process of toluene over the 3DOM-Mn1Ce2 and Mn1Ce2 catalysts at different time and temperature.

Position/cm^{-1}	Assignment	Corresponding species
1002, 1014 and 1034	C–H out-of-plane and in-plane bending vibrations	aromatic ring
1023, 1082, 1097, 1131, 1179, 1245	C–O stretching vibrations of alkoxide species	benzyl alcohol
1212	C–O stretching vibration	phenolate
1304	asymmetric C–O stretching	maleic anhydride
1444, 1455, 1494, 1595, 1607	skeletal C=C stretching vibrations	aromatic ring
1397, 1413	symmetric C–O stretching vibrations of carboxylate group	benzoate
1530, 1562	asymmetric C–O stretching vibrations of carboxylate group	benzoate
1621	C=O stretching vibration	aldehydic adsorbate
1686, 1697	C=O stretching vibration of carbonyl group	benzaldehyde
1770, 1814, 1871, 1913,1954	asymmetric and symmetric C=O stretching vibrations of cyclic anhydrides	maleic anhydride
2300-2400	the stretching vibration of CO_2	CO_2
2874 and 2924	symmetric and asymmetric C–H stretching vibrations of CH_2 group	benzyl
3028 and 3066	phenylic C–H stretching vibration	aromatic ring
3500-3600	O–H stretching vibrations	H_2O